Energy Bands in Ferromagnetic Iron*

R. A. Tawil and J. Callaway
Department of Physics and Astronomy, Louisiana State University, Baton Rouge, Louisiana 70803
(Received 30 November 1972)

Results of a self-consistent tight-binding calculation of the band structure of body-centered-cubic iron are reported. The basis set consisted of atomic wave functions for the $1s$, $2s$, $3s$, $4s$, $2p$, $3p$, and $4p$ states, expressed as linear combinations of Gaussian-type orbitals (GTO), and five individual GTO for each $3d$ state. The Coulomb part of the crystal potential in the first iteration was constructed from a superposition of overlapping neutral-atom charge densities; the atoms being in the $3d^7 4s^1$ configuration. Exchange potentials for both spins were calculated utilizing the $X\alpha$ method. Self-consistent band structures were obtained for different values of the exchange parameter α. Best results appear to be obtained for $\alpha=0.64$. In this case, 140 points in $\frac{1}{48}$ of the Brillouin zone (BZ) were used to determine the charge density. The resulting self-consistent potentials were then utilized to compute energy levels at 819 regularly spaced points in $\frac{1}{48}$ of the BZ. The results thus obtained are discussed and compared with other reported band-structure results for the same metal. The Fermi surface is analyzed in detail. The density of states has been computed. Magnetic and x-ray form factors are presented. The results are found to be in reasonably good agreement with experiment.

I. INTRODUCTION

The properties of the ferromagnetic transition metals have presented a formidable challenge to energy-band theory for more than 30 years. Iron, in particular, has been the subject of a long series of calculations employing a variety of different methods.[1-19] The continuing controversies surrounding the theory of ferromagnetism[20] sustain interest in this problem. We report here the results of the application to iron of a recently developed form of the tight-binding method[21,22] which has previously been used in a study of ferromagnetic nickel.[23,24]

A self-consistent crystal potential is obtained by an iterative procedure in which the electron distribution is sampled at 140 points in $\frac{1}{48}$ of the Brillouin zone. Separate exchange potentials are constructed for majority ($\uparrow$) and minority ($\downarrow$) spin electrons according to the $X\alpha$ method of Slater, Wilson, and Wood.[25] Spin-orbit coupling is neglected. Since this calculation offers the possibility of a detailed test of the ability of a one-electron theory with a local exchange potential to describe the electronic structure of a ferromagnetic metal, comparison is made with the results of a number of different experiments. Generally good, although not perfect, agreement with experiment is found.

The long history of calculations concerning this metal makes a brief review of previous work desirable. The early studies (Manning,[1] Callaway,[2] Suffczynski[3]) were subject to severe limitations imposed by computational facilities which were completely inadequate by present standards. The first calculation which gave a reasonably satisfactory picture of the band structure was performed by Wood[5] for paramagnetic iron using the augmented-plane-wave (APW) method. This calculation has been used to construct a density of states (Cornwell, Hum, and Wong[15]). Attempts have been made to adopt this band structure to ferromagnetic iron by the introduction of a constant spin splitting between states of majority and minority spins, and such a split-band structure has furnished a theoretical model for the interpretation of de Haas–Van Alphen data (Gold,[26] Gold *et al.*[27]). Although this procedure is not altogether unsatisfactory, our investigation shows that the spin splitting not only varies over the d band, but is substantially smaller (by a factor of 2 or more) for states of predominately s and p symmetry, as compared to those of predominately d symmetry.

Wakoh and Yamashita[8] (WY) applied the Korringa–Kohn–Rostoker (KKR) (Green's-function) method to a calculation of the band structure of ferromagnetic iron, using a spin-polarized $X\alpha$ approach to the exchange potential. Their choice of potential is similar to ours; however, there are some significant differences. In the first place, WY used an ionic Coulomb potential in each unit cell. This procedure is in the spirit of the Wigner–Seitz approximation used in the alkali metals; however, it is not consistent with the use of a local statistical $\rho^{1/3}$ exchange. WY attempted to achieve self-consistency, but it is not clear how this can be done meaningfully within the constraints imposed by a muffin-tin approximation to the crystal potential. They were also unable to sample the charge density at an adequate number of $\vec{k}$ points within the Brillouin zone. Finally, they were forced to use an interpolation scheme to obtain energy values throughout the zone. In spite of these differences, our results agree fairly well with those of Wakoh and Yamashita. Connolly[13] has reported briefly a

similar calculation using the APW method and an exchange potential due to Lindgren.[28]

Many calculations have been made using forms of the tight-binding method.[3,4,7,9,11,14,17,18] In several of these, unnecessary and stringent approximations have been made in evaluating matrix elements on the chosen basis. As one example, Abate and Asdente[7] ignore the nonorthogonality of atomic wave functions on different sites, neglect s-d by hydridization, and construct an extremely crude model potential around each site. We do not believe that quantitative results can be obtained under such restrictions.

The calculations of Stern[4] and Duff and Das[17] deserve more detailed comment. Stern modified the usual form of the tight-binding method by summing the contributions from neighboring atoms to the wave function in one cell for a state of wave vector $\vec{k}$. It is then possible to restrict integrals to a single cell. Stern used this approach to calculate the cohesive energy of paramagnetic iron in a Wigner–Seitz approximation (each cell is assumed to be neutral) and exchange was not explicitly included. His band calculation did not allow for hydridization of s and d functions, and no functions of p symmetry were included. The most important result of this work was that self-consistency was obtained for a configuration close to d^7s^1. Ingalls[9] applied Stern's approach to determine $|\psi_{4s}(0)|^2$ in order to investiate the isomer shift.

The most recent calculation concerning ferromagnetic iron is that of Duff and Das.[17,18] These authors combined tight-binding wave functions for d states with orthogonalized plane waves (the 19 OPW formed by considering the first two sets of neighbors in the reciprocal lattice). Their calculation attempts an approximate solution of the Hartree–Fock equations, and avoids the use of a statistical local-exchange potential. A static screened Coulomb potential was employed in the calculation of matrix elements of the exchange operator. Some approximations of uncertain validity were, however, employed in the band calculation: Specifically all three center integrals, and some two center integrals were neglected. Further, there is little indication that the energies of the d states have converged with the given number of OPW functions incorporated in the expansion. The d band obtained by Duff and Das is substantially wider than that found by Wood[5] or Wakoh and Yamashita.[8]

The work reported here attempts to apply the tight-binding method in a computationally adequate manner. Although a local-exchange potential is employed, the calculation is free of the limitations imposed on previous studies by approximations such as a muffin-tin potential, or incomplete convergence in the calculation of tight-binding matrix elements. The following sections contain a more detailed description of the computational procedures and results.

II. METHOD

The form of the tight-binding method employed here is a variational approach to the solution of the one-electron Schrödinger equation. A brief discussion of our procedure follows: More detailed accounts of the method have been published elsewhere.[21–23] The wave function for a state of wave vector $\vec{k}$ in band n, $\psi_n(\vec{k},\vec{r})$, is expanded in a set of basis functions $\phi_i(\vec{k},\vec{r})$, which in turn are constructed from a set of localized functions $u_i(\vec{r}-\vec{R}_\mu)$:

$$\psi_n(\vec{k},\vec{r}) = \sum_i c_{ni}(\vec{k})\phi_i(\vec{k},\vec{r}) ,$$

$$\phi_i(\vec{k},\vec{r}) = \frac{1}{N^{1/2}} \sum_\mu e^{i\vec{k}\cdot\vec{R}_\mu} u_i(\vec{r}-\vec{R}_\mu) .$$

In the present case, 38 functions u_i are considered. Thus, the Hamiltonian and overlap matrices are of dimension 38×38 at a general point of the zone. The functions for states other than $3d$ ($1s$, $2s$, $3s$, $4s$, $2p$, $3p$, $4p$) were taken from an atomic self-consistent-field calculation by Wachters.[29] These functions are linear combinations of Gaussian-type orbitals (GTO). Use of Gaussian-type orbitals is highly advantageous in tight-binding calculations; the analytic evaluation of all integrals is possible.[30] In order to describe the d-state wave functions, five radial GTO were introduced for each of the five possible $l=2$ angular functions. The exponents used in defining these functions were those employed by Wachters in his calculation for the iron atom. Since much of the disagreement between previous tight-binding band calculations probably results from the use of inaccurate wave functions (an atomic function may be either too extended or too contracted in a crystalline environment), it is desirable to incorporate sufficient flexibility in the basis set to allow the wave function to adjust to the crystal potential.

The calculation was begun by constructing a crystal potential from a superposition of overlapping neutral-atom charge densities, the atoms being assumed to be in the $3d^74s^1$ configuration. The initial spin polarization was taken as $d\uparrow^{4.61}$, $d\downarrow^{2.39}$ (s levels unpolarized). Energy levels and wave functions were determined in the potential and used to initiate an iterative procedure leading to self-consistency. In this process, corrected Fourier coefficients of the Coulomb potentials are calculated using wave functions of the occupied states resulting from the previous iteration, as has been described previously.[22]

A corrected exchange potential was obtained as follows: The change in the Fourier coefficients of charge density, for each spin, was averaged over

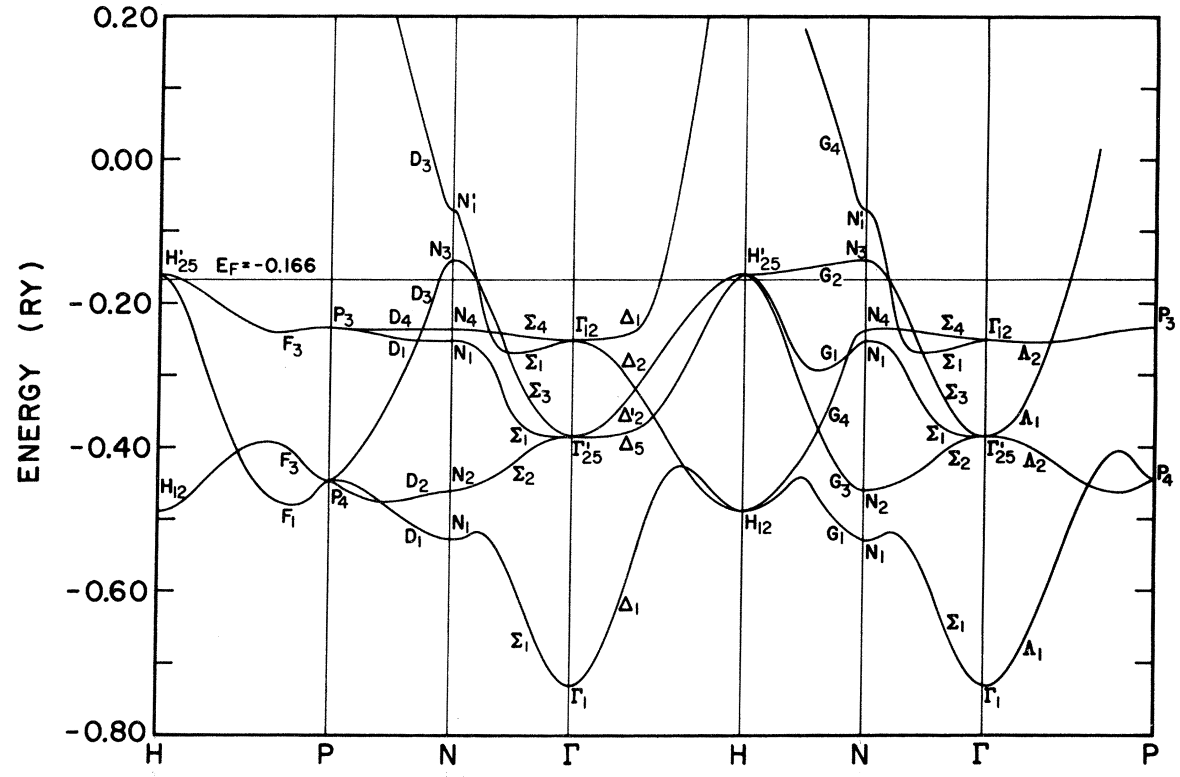

FIG. 1. Band structure for majority-spin states along certain symmetry directions. The horizontal line at 0.166 Ry indicates the Fermi energy.

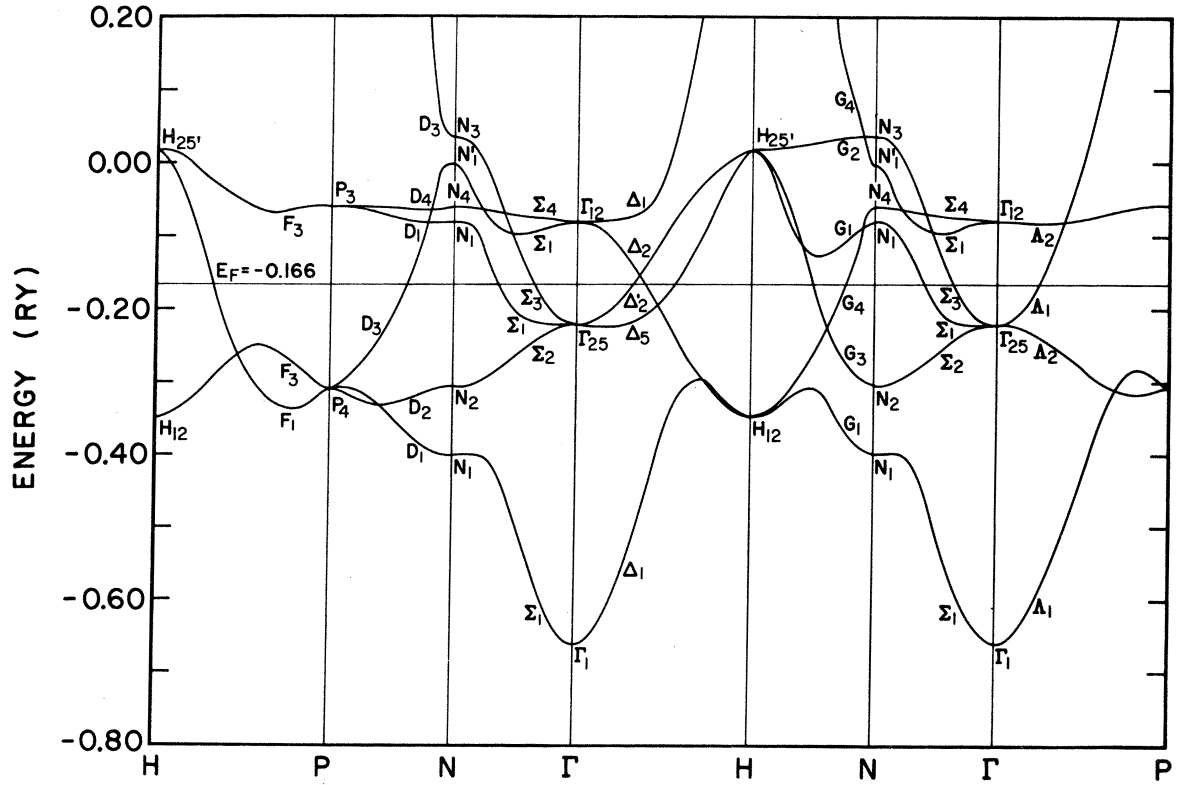

FIG. 2. Band structure for minority-spin states along certain symmetry directions.

TABLE I. Some Fourier coefficients of potential. The self-consistent Coulomb and exchange coefficients for the smallest 20 reciprocal-lattice vectors are listed. The change in these quantities resulting from the iterative process is also given.

$\vec{K}$	$V_c(K)$	$\Delta V_c(K)$	$V_{ex}\uparrow(K)$	$\Delta V_{ex}\uparrow(K)$	$V_{ex}\downarrow(K)$	$\Delta V_{ex}\downarrow(K)$
(0,0,0)	−1.6160	0.2042	−1.6842	−0.0438	−1.5223	−0.0745
(1,1,0)	−0.8220	−0.0775	−0.2907	0.0101	−0.2722	0.0155
(2,0,0)	−0.6155	−0.0289	−0.0227	0.0075	−0.0296	0.0122
(2,1,1)	−0.5000	−0.0099	−0.0325	−0.0010	−0.0356	−0.0016
(2,2,0)	−0.4221	−0.0041	−0.0555	−0.0040	−0.0539	−0.0065
(3,1,0)	−0.3651	−0.0026	−0.0467	−0.0026	−0.0444	−0.0043
(2,2,2)	−0.3213	−0.0007	−0.0224	0.0000	−0.0219	−0.0002
(3,2,1)	−0.2866	−0.0002	−0.0023	0.0016	−0.0037	0.0027
(4,0,0)	−0.2584	−0.0004	0.0054	0.0019	0.0031	0.0032
(4,1,1)	−0.2351	0.0000	0.0020	0.0010	−0.0001	−0.0019
(3,3,0)	−0.2351	0.0002	0.0020	0.0010	−0.0001	−0.0010
(4,2,0)	−0.2156	0.0002	−0.0069	−0.0002	−0.0082	0.0001
(3,3,2)	−0.1990	0.0004	−0.0157	−0.0012	−0.0162	−0.0015
(4,2,2)	−0.1847	0.0003	−0.0209	−0.0017	−0.0207	−0.0024
(5,1,0)	−0.1724	0.0001	−0.0213	−0.0016	−0.0210	−0.0023
(4,3,1)	−0.1724	0.0003	−0.0213	−0.0016	−0.0210	−0.0023
(5,2,1)	−0.1520	0.0002	−0.0125	−0.0005	−0.0127	−0.0007
(4,4,0)	−0.1436	0.0002	−0.0068	0.0002	−0.0075	0.0003
(4,3,3)	−0.1360	0.0002	−0.0025	0.0007	−0.0035	0.0010
(5,3,0)	−0.1360	0.0001	−0.0025	0.0007	−0.0035	0.0010

directions of the reciprocal-lattice vector $\vec{k}$, and the resulting Fourier series were summed numerically to determine the change in the charge density in an atomic cell. This change was added to the starting charge density of the appropriate spin; the cube root was extracted. Revised Fourier coefficients of the exchange potential were then obtained.

It was found that only the Fourier coefficients pertaining to the lowest 20 rotationally independent reciprocal-lattice vectors were appreciably affected by the self-consistent procedure. Coefficients for larger $\vec{K}$ describe the charge density inside an atomic core, and do not vary significantly. The criterion used to define an adequate degree of self-consistency was that the Fourier coefficients of the Coulomb potential should be stable to 0.001 Ry. The coefficients of the exchange potential were observed to converge somewhat more rapidly than those for the Coulomb potential.

A major problem in a calculation of this type is the determination of the optimum value of the exchange parameter α. Our previous results for nickel indicated that α should be in the neighborhood of $\frac{2}{3}$, the Kohn–Sham–Gaspar[31,32] (KSG) value.

TABLE II. Some characteristic energy differences. Our results are compared with those obtained by other authors.

	This calculation	Wakoh and Yamashita[a]	Duff and Das[b]	Wood[c]
$(H_{12}-H_{25})\uparrow$	0.33	0.35	0.74	0.44
$(H_{12}-H_{25})\downarrow$	0.37	0.39		
$(\Gamma_1-\Gamma_{25})\uparrow$	0.35	0.40	0.58	0.33
$(\Gamma_1-\Gamma_{25})\downarrow$	0.44	0.49		
$(\Gamma_{12}-\Gamma_{25})\uparrow$	0.13	0.11	0.23	0.12
$(\Gamma_{12}-\Gamma_{25})\downarrow$	0.14	0.11		
$(P_4-P_3)\uparrow$	0.21	0.18	0.45	0.25
$(P_4-P_3)\downarrow$	0.25	0.22		

[a]Reference 8. De Cicco and Kitz, Ref. 38, agree with the results of Wakoh and Yamashita.
[b]Reference 17. No values for spin↓ have been supplied.
[c]Reference 5. Paramagnetic iron.

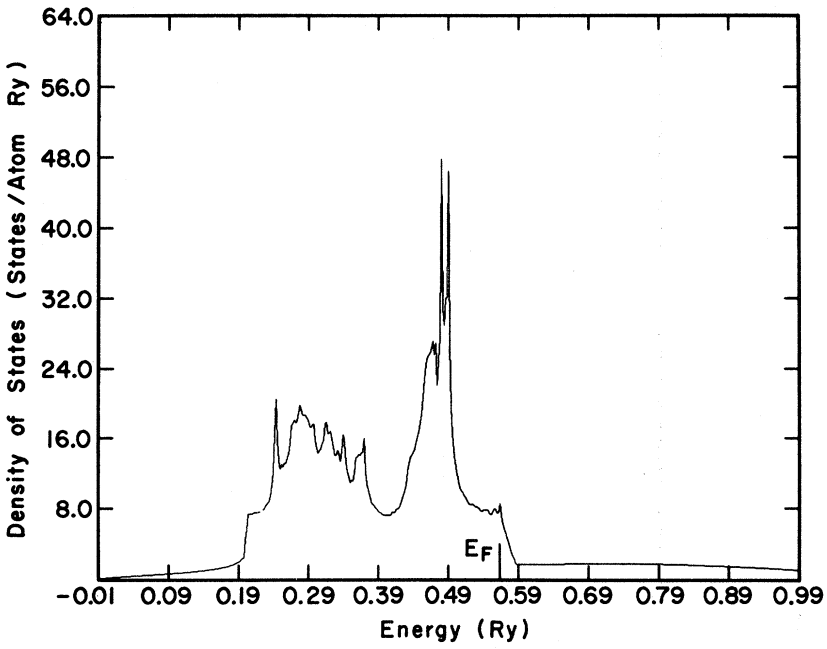

FIG. 3. Density of states of majority spin. The origin of the energy scale has been shifted arbitrarily.

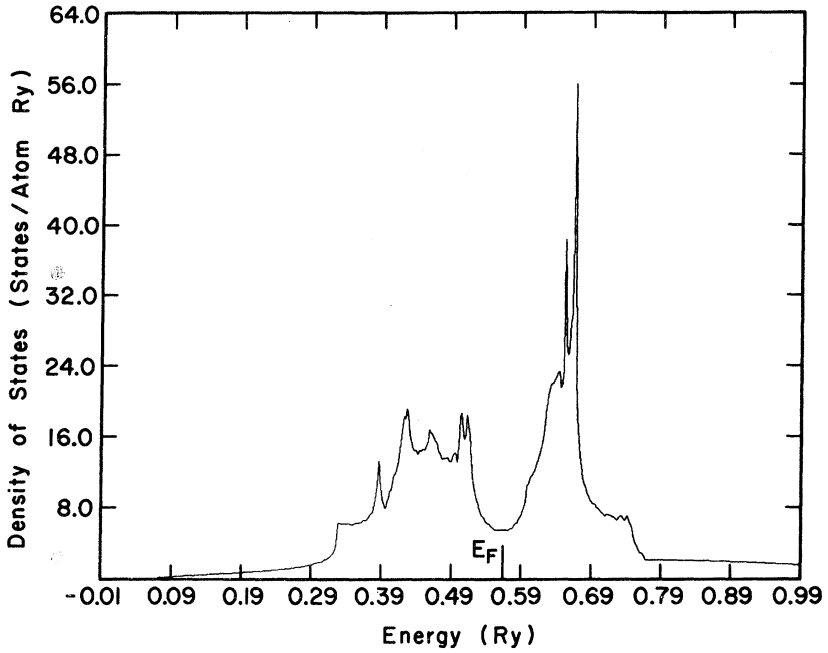

FIG. 4. Density of states of minority spin.

Complete self-consistent calculations involving a limited number of points (14 in $\frac{1}{48}$ of the zone), were made for several values of α ($\frac{2}{3}$, 0.64, 0.62, 0.60). A specific choice was made after considering the magneton number and the nature of the Fermi surface. The KSG value yielded a magneton number of 2.32 and a Fermi energy above the $H_{25'}$ level. However, the de Haas–van Alphen measurements of Gold *et al.*[27] indicate the presence of pockets of majority-spin holes associated with this state. For $\alpha = 0.60$ and 0.62, magneton numbers of 1.96 and 2.10 were obtained; hole pockets were present around H, but the areas were too large in comparison with experiment. Reasonably good results for the magneton-number and hole-pocket areas were obtained for $\alpha = 0.64$. A detailed analysis of results for this value of α will be presented in Secs. III–VI.

The final iterations of the self-consistency procedure were made using 140 points in $\frac{1}{48}$ of the

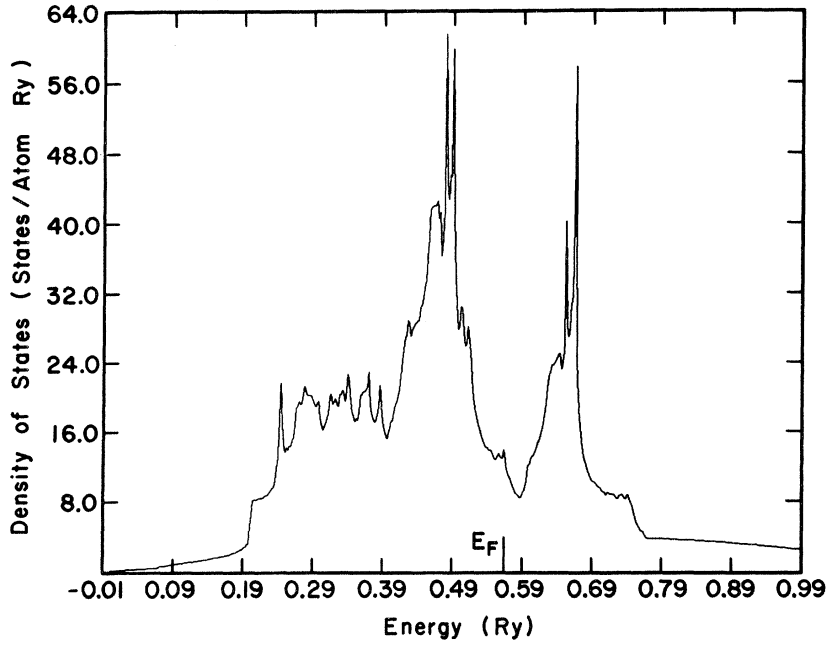

FIG. 5. Total density of states.

TABLE III. Some energy values and spin splittings at points of high symmetry.

Point	↑ Spin	↓ Spin	Splitting
Γ_1	−0.730	−0.659	0.071
$\Gamma_{25'}$	−0.385	−0.221	0.164
Γ_{12}	−0.251	−0.080	0.171
H_{12}	−0.490	−0.035	0.455
$H_{25'}$	−0.160	+0.0019	0.179
P_4	−0.446	−0.307	0.139
P_3	−0.234	−0.059	0.175
N_1	−0.528	−0.400	0.128
N_2	−0.460	−0.305	0.155
N_1	−0.253	−0.081	0.172
N_4	−0.234	−0.062	0.172
N_3	−0.140	+0.0040	0.180
$N_{1'}$	−0.070	−0.002	0.068

Brillouin zone (BZ) (and $\alpha = 0.64$). Table I shows the effect of the iterative procedure on some Fourier coefficients of the potential. After the self-consistent potential had been determined to the desired accuracy, energies were computed at 819 points in $\frac{1}{48}$ of the BZ. The density of states was computed by the Gilat–Raubenheimer method.[33] Additional calculations of energy levels were made at points close to the Fermi surface.

III. RESULTS: BAND PROPERTIES

The calculated band structure is shown in Figs. 1 and 2 for states of majority (↑) and minority (↓) spin. The bands show the expected hybridization between a narrow-d-band complex and a broad s-p band. Certain characteristic energy differences are listed in Table II, where they are compared with corresponding results of Wakoh and Yamashita,[8] Duff and Das,[17] and Wood.[5] Our values are in rough agreement with those of Wakoh and Yamashita, and Wood, but are substantially smaller, by a factor close to 2, than those of Duff and Das.

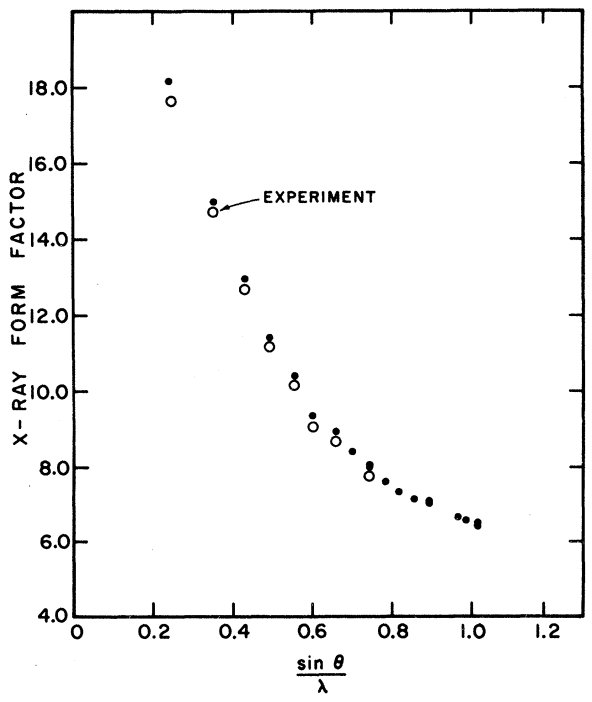

FIG. 6. Magnetic form factor $f(\vec{\kappa})$. The experimental points are from Ref. 39.

TABLE IV. Magnetic form factor.

Scat. Vector	Core	Spin	Total[a]	Experiment[b]
(0,0,0)	0.0000	2.1782	1.000	1.000
(1,1,0)	0.0056	1.3641	0.599	0.629
(2,0,0)	0.0060	0.8918	0.393	0.404
(2,1,1)	0.0050	0.5392	0.234	0.250
(2,2,0)	0.0038	0.3574	0.158	0.164
(3,1,0)	0.0024	0.3036	0.134	0.137
(2,2,2)	0.0018	0.1219	0.053	0.061
(3,2,1)	0.0011	0.1007	0.045	0.046
(4,0,0)	0.0006	0.1684	0.075	0.070
(4,1,1)	0.0002	0.0947	0.042	0.037
(3,3,0)	0.0002	0.0312	0.013	0.013
(4,2,0)	−0.0000	0.0478	0.020	0.020
(3,3,2)	−0.0002	−0.0334	−0.016	−0.016
(4,2,2)	−0.0003	−0.0179	−0.008	−0.010
(5,1,0)	−0.0004	0.0574	0.025	0.028
(4,3,1)	−0.0004	−0.0268	−0.012	−0.013
(5,2,1)	−0.0004	0.0017	0.001	0.001
(4,4,0)	−0.0004	−0.0417	−0.019	0.015
(4,4,3)	−0.0004	−0.0684	−0.030	0.027
(5,3,0)	−0.0004	−0.0244	−0.011	−0.011

[a]Total = $(2/g\mu)f_{\text{spin}}(\vec{K}) + (1/\mu)f_{\text{core}}(K)$. g = spectroscopic splitting factor, μ = magneton number. This calculation is based on a magneton number 2.1782 obtained from a histogram estimation of the density of states, rather than the more accurate value obtained in Sec. III.

[b]Reference 39.

Some specific energies and exchange splittings are presented in Table III. The predominately d states are split by approximately 2 eV; the s and p states by 1 eV or less. There is a tendency for spin splitting to increase with energy. Our results for the d-band splitting are substantially smaller (~ 60%) than those obtained by Duff and Das. The order of levels we obtain at N differs from that found by Wood in regard to the location of the predominately p-like level $N_{1'}$. Our results agree with those of Wakoh and Yamashita in this regard.

The densities of states for the majority and minority spins, and their combinations, are shown in Figs. 3–5. A high sharp structure is to be noted near the top of the d bands. A somewhat similar structure is found in nickel. The peak here results from a nearly flat band of predominately e_g symmetry ($\Gamma_{12} - \Sigma_4 - N_4 - D_4 - P_3$). Although the single-spin densities of states are similar in appearance,

they are not identical. The d-band portion of the majority-spin density of states is somewhat wider (by approximately 0.7 eV) than that of the minority spins. In addition, the peak and valley structure is different; the minority spins have a higher peak and lower valley than the majority spins. These remarks indicate that the exchange splitting of the band structure should not be considered as a rigid shift.

The combined density of states shows a pronounced two-peak structure, which is primarily a consequence of the exchange splitting. The Fermi energy falls in the region of the minimum between the peaks. The width of the occupied portion of the d-band part of the density of states measured from the onset of the rapid increase at low energy to the Fermi energy is 5.0 eV. This is consistent with the observations of Fadley and Shirley.[34] The density of states at the Fermi energy is, for majority spin, 7.52/atom Ry, and for minority spin, 5.65/atom Ry. This yields an electron-specific-heat coefficient

$$\gamma = \tfrac{1}{3}\pi^2 N(E_F) K^2 = 2.28\times10^{-3}\ \text{J/mole °K}^2 .$$

A recent experimental result for this quantity is 4.74×10^{-3} J/mole °K^2.[35] A portion of the discrepancy can probably be attributed to effects of the electron-phonon interaction. The occupation number for majority spin is 5.13; for minority spin, 2.87. The resulting magneton number, 2.26 electrons per atom, is in good agreement with the experimental value of 2.21. Our results in this respect are superior to those of Connolly.[13]

IV. SPIN DENSITY

The distribution of the spin density in iron has been studied by neutron-diffraction techniques.[36,37] Such an experiment determines a magnetic form factor $f(\vec{\kappa})$ which is the ratio of the magnetic scattering amplitude for a scattering vector $\vec{\kappa}$, to that for $\vec{\kappa}=0$. It has become customary to express $f(\vec{\kappa})$ as the sum of three terms,

$$f(\vec{\kappa}) = (2/g) f_{\text{spin}}(\vec{\kappa}) + f_{\text{core}}(\vec{\kappa}) + [(g-2)/g] f_{\text{orb}}(\vec{\kappa}) ,$$

in which g is the spectroscopic splitting factor, equal to 2.12 for iron. The quantity f_{spin} is the form factor for the unpaired (mainly d) electrons, and is normalized so that $f_{\text{spin}}(0)=1$,

$$f_{\text{spin}}(\kappa) = (N\nu)^{-1} \int e^{i\vec{\kappa}\cdot\vec{r}} [\rho_\uparrow(\vec{r}) - \rho_\downarrow(\vec{r})]\, d^3r ,$$

in which ν is the magneton number. Although the core has a net spin of zero, exchange effects produce a slight difference in the radial distributions of $\uparrow$ and $\downarrow$ spin electrons, and so lead to a small contribution f_{core}. Finally, there is a contribution f_{orb} from the possible unquenched orbital angular momentum of the d electron.

TABLE V. X-ray-scattering form factor.

Scat. Vector	Calc. Core	Calc. Total	Experiment
(1,1,0)	15.138	18.38	17.63 ± 0.20
(2,0,0)	13.135	15.08	14.70 ± 0.23
(2,1,1)	11.69	13.04	12.62 ± 0.21
(2,2,0)	10.616	11.55	11.13 ± 0.20
(3,1,0)	9.802	10.42	10.10 ± 0.19
(2,2,2)	9.173	9.62	9.13 ± 0.25
(3,2,1)	8.677	8.98	8.75 ± 0.10
(4,0,0)	8.277	8.45	
(3,3,0)	7.950	8.06	7.68 ± 0.21
(4,1,1)	7.950	8.08	7.68 ± 0.21

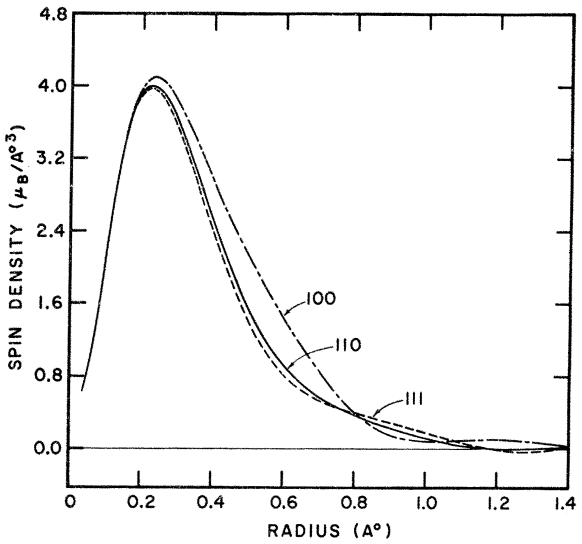

FIG. 7. Position dependence of the spin density in three crystallographic directions.

The magnetic form factor for iron has been computed theoretically by De Cicco and Kitz,[38] and by Duff and Das.[18] We have calculated the spin and core contribution to $f(\kappa)$. The orbital contribution f_{orb} is zero under the present approximations in which spin-orbit coupling is neglected. The results are tabulated in Table IV, and are shown graphically in Fig. 6. The comparison with experiment[39] is quite satisfactory. It should be noticed that the spin density is not spherically symmetric [compare $f(\kappa)$ for $k=411$ and 330; 510 and 431, 433 and 530]. The deviation from spherical symmetry is also consistent with experiment.

It is of interest to examine the position dependence of the spin density. This is shown for three different directions in Fig. 7. A small negative spin polarization is obtained well away from the nucleus in the [110] and [111] directions.

TABLE VI. Enumeration and description of sheets of Fermi surface.

	Majority (↑)	
I	Large electron surface about Γ	Approximately spherical with distortions along 12 bulges along the [110].
II	Major hole surface about H	12 long arms extending along H to N directions. 8 deep funnellike indentations along [111] and intersects III along [111]. Six indentations along [100]. 24 bulges in the $k_x=k_y$ planes centered about the directions (8, 3, 3). Does not intersect I.
III	Intermediate hole pocket about H	Fits inside II and has eight sharp points of contact with II along [111]. Touches IV tangentially at six points along [100].
	Minority (↓)	
IV	Minor hole pocket about H	Fits inside III, with which it has six tangential points of contact along [100].
V	Large hole surface about H	Approximately octahedral. Contacts VII(a) at six points along [100]
VI(a)	Large electron surface about Γ	Approximately octahedral. No intersections with V or VII(a).
VII(a)	Electron ball along Δ	Ball has six tangential points of contact with V along [100].
VIII	Hole pocket at N	Approximately ellipsoidal and does not intersect V, VI(a), or VII(a).

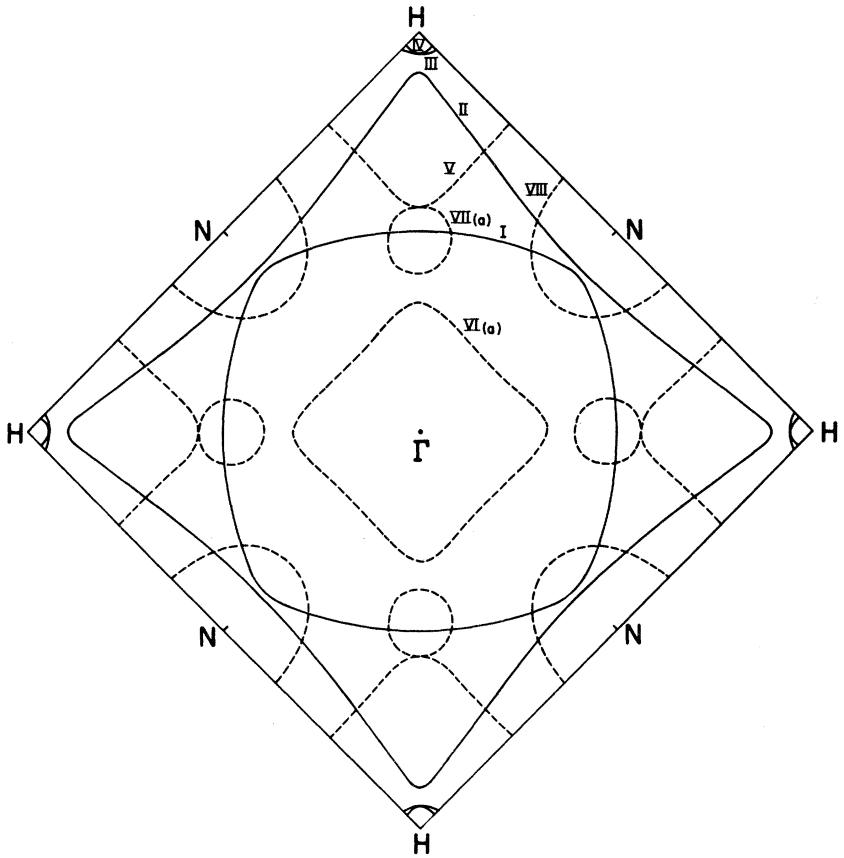

FIG. 8. Fermi-surface cross sections in the (100) plane.

V. CHARGE DENSITY

We have related the calculated charge distribution to experiment through a computation of the x-ray atomic-scattering form factor. This quantity has been measured by Batterman, Chipman, and De Marco.[40] Our results are presented and compared with experiment in Table V. There is only a moderate degree of agreement, as the theoretical results appear to be consistently larger than the experimental values by 3–5%. In view of the fact that the experimental values lie significantly below the calculated core contribution at large $\vec{K}$ it is possible that the errors in the experiment have been underestimated.

Some evidence that the charge distribution departs from spherical symmetry is seen in that $f(330) \neq f(411)$. The ratio of these quantities has been measured by De Marco and Weiss[41] to be

$$f^2(330)/f^2(411) = 1.023 \pm 0.005 .$$

We obtain

$$f^2(330)/f^2(411) = 1.005 .$$

VI. FERMI SURFACE

Information concerning the Fermi surface of iron is derived from studies of magnetoresistance[42–44] and the de Haas–van Alphen effect.[27] These measurements are of great importance in that they indicate that a model of the electronic structure of iron involving localized $3d$ electrons and itinerant $4s$ electrons is untenable. Instead, the Fermi surface has components in the d-band complex. We have studied the Fermi surface which results from

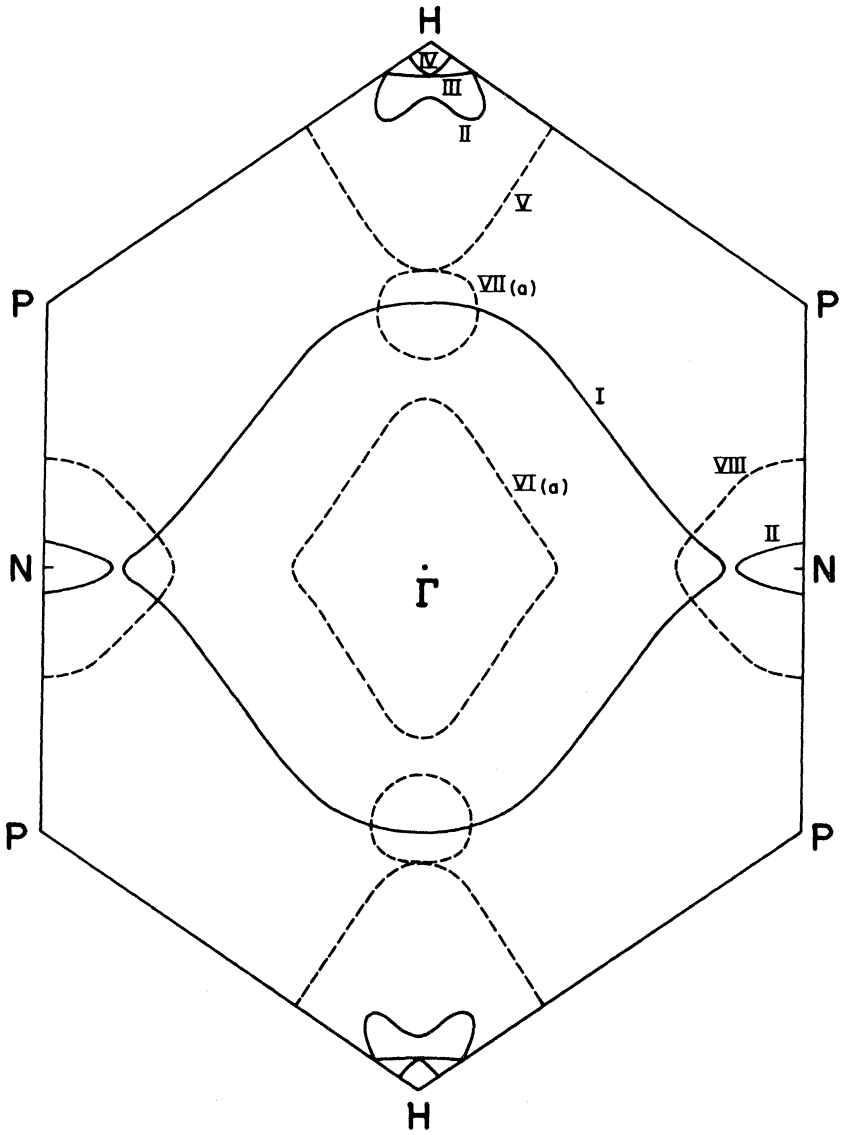

FIG. 9. Fermi-surface cross sections in the (110) plane.

TABLE VII. Predicted de Haas–van Alphen frequencies in MG are compared with Gold's model A and with experiment (Ref. 27).

Plane		This calculation	Model A (Gold, 1971)	Experiment (Gold, 1971)
(1, 0, 0)				
	I	421	436	not reported
	III	5.5	17.6	5.05 ± 0.03
	IV	4.6	15.4	3.88 ± 0.02
	V	219	219	unobserved
	VI(a)	119.2	63	unobserved
	VII(a)	11.01	6.5	21.0 ± 0.1
	VIII	71.9	absent	unobserved
(1, 1, 0)				
	I	347	358	347 ± 5
	II (around *N*)	8.4	absent	unobserved
	II (around *H*)	20.3	absent	unobserved
	III	8.17	27	unobserved
	IV	3.72	15	3.9 ± 0.03
	V	171.8	168	unobserved
	VI(a)	91.8	54	unobserved
	VII(a)	12.4	6.5	12.0 ± 0.2
	VIII	70.1	absent	unobserved
(1, 1, 1)				
	I	370	372	369 ± 4
	II	27.8	434	28.0 ± 0.2
	III	9.9	21.9	11.3 ± 0.2
	IV	4.4	12.4	4.13 ± 0.03
	V	162	145	154 ± 1
	VI(a)	69.4	49	unobserved
	VIII Γ	64.8	absent	unobserved
	VIII *H*	60.2	absent	51.8 ± 0.6

our calculation. Our conclusions are summarized in Tables VI and VII, and cross sections are shown in Figs. 8–10. No attempt has been made to obtain a precise fit to the experimental cross sections through semiempirical interpolation methods.

The Fermi surface has components in majority- and minority-spin bands. The different sheets of Fermi surface are listed in Table VI, which may be compared with a similar enumeration by Gold *et al.*[27] The portions belonging to majority-spin electrons include a large electron surface about Γ. This is roughly spherical with some bulges along the [110] axis in the direction of *N*. This, and the corresponding smaller minority-spin electron surface about Γ, are all that would be expected if a localized model of the *d* electrons were correct. However, in addition there is a major surface of majority-spin holes with long arms running around the face of the zone, *H-N-H*, etc. These arms provide the possibility of open orbits, as observed in magnetoresistance experiments. Two smaller hole pockets around *H* complete the majority-spin surface.

The minority-spin portion of the Fermi surface contains relatively large octahedral hole surfaces around *H* and electron surfaces around Γ. These pieces somewhat resemble the predicted Fermi surface of a paramagnetic form of chromium. In addition, we predict the existence of electron balls along the [100] axes, touching the hole surface, and moderately large hole pockets around *N*. The large surfaces around Γ and *H* are predicted in all calculations; however, differences exist in regard to other portions. For example, Wakoh and Yamashita obtain an electron jack touching the surface about Γ, rather than the ball mentioned above.

In order to facilitate comparison with experiment, we present in Table VIII computed de Haas–Van Alphen frequencies for cross sections of the Fermi surface in the (100), (110), and (111) planes. The surfaces are those described in Table VI. The relation between frequency (in MG) and area is $F = 505\,a$,[27] in which a is measured in units of $(2\pi/a)^2$,

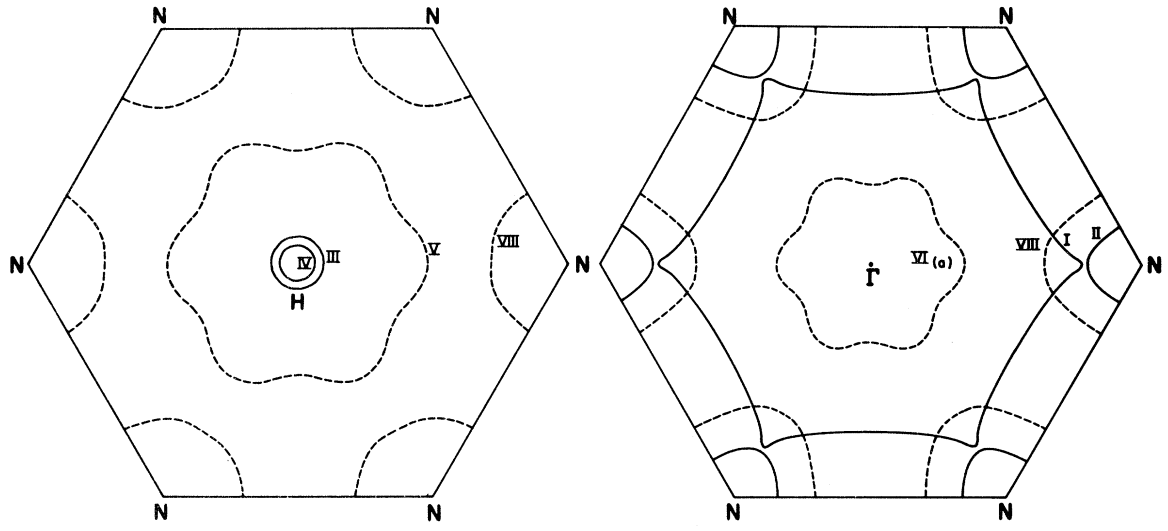

FIG. 10. Fermi-surface cross sections in (111) planes.

a being the low-temperature lattice constant. We have correlated our values with Gold's semiempirical-model A where possible.[27] We have also quoted the experimental frequencies in cases where the identification of an oscillation seemed to be clear.

The results seem to be quite satisfactory for the large electron surface I, and for the hole pockets around H. Some of the other cross sections match quite well; however, there are many more predicted pieces of the Fermi surface than are actually observed. We have also been unable to identify a small number of oscillations observed by Gold *et al*. The problem is, of course, complicated by spin-orbit coupling which breaks many of the degeneracies between majority- and minority-spin bands, and introduces small gaps which may be subject to magnetic breakdowns. Additional open orbits, relevant to magnetoresistance observations, may be introduced. We plan further calculations to investigate in detail the effects of spin-orbit coupling.

---

*Supported in part by the U. S. Air Force Office of Scientific Research.

[1]M. F. Manning, Phys. Rev. **63,** 190 (1943).
[2]J. Callaway, Phys. Rev. **99,** 500 (1955).
[3]M. Suffczynski, Acta Phys. Pol. **16,** 161 (1957).
[4]F. Stern, Phys. Rev. **116,** 1399 (1959).
[5]J. H. Wood, Phys. Rev. **126,** 517 (1962).
[6]L. F. Mattheiss, Phys. Rev. **134,** A970 (1964).
[7]E. Abate and M. Asdente, Phys. Rev. **140,** 1303 (1965).
[8]S. Wakoh and J. Yamashita, J. Phys. Soc. Jap. **21,** 1712 (1966).
[9]R. Ingalls, Phys. Rev. **155,** 157 (1967).
[10]M. Asdente and M. Delitala, Phys. Rev. **163,** 497 (1967).
[11]S. Kobayasi and S. Matumoto, J. Phys. Soc. Jap. **22,** 933 (1967).
[12]J. Hubbard and N. W. Dalton, J. Phys. C **1,** 1637 (1968).
[13]J. W. D. Connolly, Int. J. Quantum Chem. **2,** 5257 (1968).
[14]V. P. Shirokovskiy and Z. V. Kulakova, Fiz. Met. Metalloved. **25,** 404 (1968) [Phys. Met. Metallogr. **25,** 20 (1968)].
[15]J. F. Cornwell, D. M. Hum, and K. C. Wong, Phys. Lett. A **26,** 365 (1968).
[16]D. M. Hum and K. C. Wong, J. Phys. C **2,** 833 (1969).
[17]K. J. Duff and T. P. Das, Phys. Rev. B **3,** 1921 (1971).
[18]K. J. Duff and T. P. Das, Phys. Rev. B **3,** 2294 (1971).
[19]L. Kleinman and R. Shurtleff, Phys. Rev. B **4,** 3284 (1971).
[20]C. Herring, *Exchange Interactions Among Itinerant Electrons* (Academic, New York, 1966).
[21]E. Lafon and C. C. Lin, Phys. Rev. **152,** 597 (1966).
[22]J. Callaway and J. L. Fry, in *Computational Methods in Band Theory*, edited by P. M. Marcus, J. F. Janak, and A. R. Williams (Plenum, New York, 1971), p. 571.
[23]J. Langlinais and J. Callaway, Phys. Rev. B **5,** 124 (1972).
[24]J. Callaway and C. S. Wang, Phys. Rev. B 7, 1096 (1973).
[25]J. C. Slater, T. M. Wilson, and J. H. Wood, Phys. Rev. **179,** 28 (1969).
[26]A. V. Gold, J. Appl. Phys. **163,** 497 (1967).
[27]A. V. Gold, L. Hodges, P. T. Panousis, and D. R. Stone, Int. J. Magn. **2,** 357 (1971).
[28]I. Lindgren, Phys. Lett. **19,** 382 (1965); Ark. Fys. **31,** 59 (1966).
[29]A. J. H. Wachters, J. Chem. Phys. **52,** 1033 (1970).
[30]R. C. Chaney, T. K. Tung, C. C. Lin, and E. Lafon, J. Chem. Phys. **52,** 361 (1970).
[31]W. Kohn and L. J. Sham, Phys. Rev. **140,** A1133 (1965).
[32]R. Gaspar, Acta Phys. **3,** 263 (1954).
[33]G. Gilat and L. J. Raubenheimer, Phys. Rev. **144,** 340 (1966).
[34]C. S. Fadley and D. A. Shirley, J. Res. Natl. Bur. Stand. (U.S.) A **74,** 543 (1970).
[35]M. Dixon, F. E. Hoare, T. M. Holden, and D. E. Moody, Proc. R. Soc. A **285,** 561 (1965).
[36]C. G. Shull, in *Electronic Structure and Alloy Chemistry of the Transition Elements*, edited by P. A. Beck (Wiley, New York, 1963), p. 69.
[37]C. G. Shull and H. A. Mook, Phys. Rev. Lett. **16,** 184 (1966).
[38]P. D. DeCicco and A. Kitz, Phys. Rev. **162,** 486 (1967).
[39]C. G. Shull, quoted by P. D. De Cicco and A. Kitz, in Ref. 36.
[40]B. W. Batterman, D. R. Chipman, and J. J. De Marco, Phys. Rev. **122,** 68 (1961).
[41]J. J. De Marco and R. J. Weiss, Phys. Lett. **18,** 92 (1965).
[42]W. A. Reed and E. Fawcett, Phys. Rev. **136,** A422 (1964).
[43]A. Isin and R. V. Coleman, Phys. Rev. **137,** A1609 (1965).
[44]W. A. Reed and E. Fawcett, in *Proceedings of the International Conference on Magnetism, Nottingham, 1964* (The Institute of Physics and Physical Society, London, 1965), p. 120.